Proceedings of the 17th World Congress
The International Federation of Automatic Control
Seoul, Korea, July 6-11, 2008

Analysis of changes in the beat-to-beat P-wave morphology using clustering techniques

Alberto Herreros (albher@eis.uva.es) *
Enrique Baeyens (enrbae@eis.uva.es) *
Jonas Carlson (Jonas.Carlson@kard.lu.se) ***
Rolf Johansson (Rolf.Johansson@control.lth.se) **
José R. Perán (peran@eis.uva.es) *
Bertil Olsson (Bertil.Olsson@med.lu.se) ***

* *Department of Systems Engineering and Automatic Control. University of Valladolid, Spain.*
** *Department of Automatic Control. LTH. Lund University, Sweden.*
*** *Department of Cardiology. University Hospital. Lund University, Sweden.*

Abstract: Several pathologies related to the atrial electrical activity can be detected in the electrocardiogram P-wave. A study on the beat-to-beat P-wave morphology changes of 89 ECG signals is performed in this article. An algorithm based on the embedding space techniques has been used to extract the P-wave information of the ECG. The P-waves obtained in several of these ECGs exhibit intermittent morphology changes. The morphologies have been classified by using the K-means clustering algorithm. The mechanism behind different P-wave morphologies and its possible pathophysiological importance remains to be clarified.

Keywords: P-wave morphology, K-means clusters, ECG wave delineation, atrial electrical activity.

1. INTRODUCTION

The interatrial conduction delay is considered as one of the causes of several atrial pathologies. The normal cardiac rhythm is initiated in the sinus node, and is propagated along the entire atrial myocardium. There are three internodal conduction pathways in the right atrium and multiple potential interatrial paths. Atrial conduction disorders frequently appear in elderly or structural heart disease subjects and can be the origin of the atrial fibrillation, flutter or tachyarrhythmias, see Daubert et al. [2004].

The analysis of the electrocardiogram (ECG) is a well-known non-invasive technique to detect the electrical heart activity. A normal heart cycle is reflected in the ECG by a P-wave (atrial activity), a QRS complex and a T-wave. Several clinical studies connect certain P-wave properties such as its length and morphology, with anomalies in the electrical atrial conduction and atrial pathologies, see Daubert et al. [2004], Platonov et al. [2000, 1998], Hävmoller et al. [2007], Carlson et al. [2005] The relationship between P-wave indices, measured with Frank leads, and atrial fibrillation is studied in Platonov et al. [2000, 1998]. The length of the P-wave, the time position of the X-lead peak and the sign of the Z-lead signal value are some of the most frequently used indices to predict atrial anomalies.

⋆ This work was supported in part by the national research agency of Spain (CICYT) through the project DPI 2006-14367 and the regional government of Castilla y León through the project VA076A07.

The P-wave morphology of 89 orthogonal ECG signals belonging to both healthy individuals and patients with intermittent atrial rhythm disorders is studied here. The aim is to analyze the P-wave morphology, using the indices and criteria proposed by Platonov et al. [2000], to detect possible interatrial conduction delays. Similar indices have been used by Censi et al. [2007] to analyze the relationship between the P-wave morphology and the atrial fibrillation.

The magnitude and length of the P-waves are smaller than those of the QRS complexes and T-waves, and their study requires more sophisticated computation techniques. The ECG baseline oscillations, due to the respiratory cycle, and the high frequency noise have, in some cases, the same magnitude as the P-wave and could hide or disturb it. Most ECG detection algorithms only detect the QRS complexes, see Köhler et al. [2002], Sörnmo and Laguna [2005]. Other algorithms try to obtain all the characteristic points of the ECG, *i.e.*, the onset, peak and end of the P-waves, QRS complexes and T-waves. Several mathematical tools, such as wavelets, see Martinez et al. [2004], Bahoura et al. [1997], Li et al. [1995], Sahambi et al. [1997], or hidden Markov chains, see Koski [1996], have been employed. These methods are based on estimation techniques, where a reference wave is compared to the actual signal in different time and/or frequency spaces.

The criteria applied by a professional cardiologist in order to locate the characteristic event point positions vary. The P-wave onset is normally defined as the start of this wave

in one of their leads, and the P-wave end is defined in some articles as the "nadir location", *i.e.*, an inverse peak in the spatial magnitude, see Platonov et al. [2000].

The algorithm proposed by Herreros et al. [2007] is used to detect and extract the P-waves from ECG records. This algorithm avoids the abovementioned difficulties associated to the detection of P-wave characteristic events and is based on the embedding phase-space of a measured signal, see Kantz and Schreiber [1997], Abarbanel [1996, 1993]. The algorithm transforms the ECG lead time signal in a sequence of points of a new multidimensional space. Its performance has been tested using both simulated and true ECG signals.

The P-wave information was extracted from 89 ECG signals to obtain the indices proposed in Platonov et al. [2000]. It has been checked that 18 of these ECG signals have significant changes in the beat-to-beat P-wave morphology. Since the indices in Platonov et al. [2000] are computed on the average of all the P-waves, the morphology change information is lost. In order to avoid this, a classification method to assort the morphologies (including beat-to-beat information) from an ECG signal is developed. The mathematical tool employed for classification was the K-means clustering algorithm, see Bezdek and Pal [1992], Duda et al. [2001], that allows a choice in the number of the required classification sets. Other classification approaches such as neural nets could be applied, see Bishop [1997]. However the K means algorithm is faster, easier to implement and does not require a training phase.

The characteristic indices proposed by Platonov et al. [2000] have been computed for each resultant P-wave morphology for the 89 cases of this study. In some cases, a large variation in the indices from one to the other morphology occurs. This can be associated to a change in the atrial electrical conduction.

The rest of this paper is organized as follows: Section 2 introduces the main tools employed for this research study, namely, the phase-space detection algorithm, the K-means clustering technique and the characteristic indices for the P-wave morphology study. Section 3 explains the protocol to extract the P-wave information from the ECG signals and the classification of the P-wave morphologies and presents the results, that are discussed later in Section 4. Finally, some conclusions are summarized in Section 5.

2. DESCRIPTION OF MATERIALS AND METHODS

2.1 Data acquisition

The surface ECG was sampled during normal heart rhythm (sinus rhythm) using modified Frank leads (X, Y and Z) at a rate of 1 kHz and a resolution of $0 - 625$ μV, using a special software and a data acquisition board (equipment supplied by Siemens-Elema AB, Solna, Sweden). The X lead was applied to the fourth intercostal space in both mid-axillary lines; the Y lead at the sternal manubrium, just below the clavicle, and to the left of the fifth of the umbilicus; and the Z lead at the fifth intercostal space and on the spinal backbone.

The ECG data collection was obtained at the Cardiology Department of the Lund University. The number of studied ECGs was 89, most of them being recorded from healthy people. The patient were at rest during the record of 6 minutes.

2.2 Phase-space detection algorithm.

An algorithm based on the embedding phase-space approach to detect the characteristic points of an ECG and was developed. The multi-lead ECG was mapped into points of an embedding phase space, in such a way that similar ECG morphologies are converted into phase-space points that are close in some distance measure. The algorithm was characterized by three parameters, the delay δ, the embedding dimension N and a vector of integer numbers that depends on the relative position of the reference point in the wave under study, $\beta \in \mathbb{R}^{N+1}$, see the details in Herreros et al. [2007]. The algorithm can be applied to different characteristic points (onset, peak and end) and is robust against morphology changes, baseline oscillations and high frequency noise. Its performance was succesfully validated using both simulated and real ECG signals.

2.3 Cluster analysis

Several techniques can be used to classify data into a finite number of classes with similar properties, see Bezdek and Pal [1992], Duda et al. [2001]. Clustering methods classify data by using a data distance. The data are represented as a collection of vectors $S = \{x_1, \ldots, x_L\}$ in a finite dimension feature space $S \subset \mathbb{R}^N$ and the data distance can be any vector norm in that space, usually the Euclidean norm of $\mathbb{R}^N$. The K-means clustering method is one of the simplest procedures for solving the problem of classifying L data points $\{x_1, \ldots, x_L\}$ in K different clusters C_i, $i = 1, \ldots, K$. Each cluster was characterized by a centroid that is the barycenter of all the points in the cluster, *i.e.* the point that minimizes the sum of the distances of all the points of the cluster to it. The method aimed at minimizing an objective function, in this case the squared error function

$$J = \sum_{i=1}^{K} \sum_{j \in C_i} ||x_j - \mu_i||^2 \tag{1}$$

where C_i is the ith cluster and $\|x_j - \mu_i\|^2$ is the square of the distance from the data point $x_j \in C_i$ to the centroid μ_i of the cluster C_i. A summary of the K-means clustering algorithm is given in Table 1. It has been proved that the algorithm converges, however the computed solution need not be the global optimum. In fact, the algorithm is quite sensitive to the initial locations of the centroids and could be run multiple times with different initial centroids in order to reduce this effect.

The K-means clustering technique has been employed as a tool for classifying the different ECG signals in groups depending on the P-wave morphology. After a detailed analysis of 89 real ECG signals, it was checked that 18 individuals present beat-to-beat P-wave morphology changes in their ECGs.

2.4 P-wave morphology indices

The P-wave morphology analysis can be used to predict several atrial pathologies, such as atrial fibrillation, see

Table 1. K-Means clustering algorithm

(1) Place the initial group of centroids $\{\mu_1, \mu_2, \ldots, \mu_K\}$ in the space $\mathbb{R}^N$.
(2) Assign each object x_i, $i = 1, \ldots, L$ to the group that has the closest centroid.
(3) Recalculate de position of the centroids by computing the barycenter of each cluster $\mu_i = \min \sum_{j \in C_i} ||x_j - \mu_i||^2$, $i = 1, \ldots, K$.
(4) Repet step 2. and 3. until the centroids no longer move.

Platonov et al. [2000, 1998], Carlson et al. [2001]. These authors use the Frank leads X, Y, Z and the spatial magnitude SM, defined as $SM = \sqrt{X^2 + Y^2 + Z^2}$, to predict pathologies. In addition, they define some indices in order to show that the delay in the interatrial conduction of the P-wave is a predictor of some atrial pathologies. The most commonly used indices to analyze the P-wave morphology are: its length, the time of the maximum X and Y peaks, the Z cross-zero time, the minimum and maximum Z peak magnitudes and the peaks of the spatial magnitude SM. For example, a large maximum Z peak and the presence of two peaks in the SM signal may indicate an interatrial delay.

A new index that measures the degree of variability of the ECG P-wave morphology is proposed here. The index of change is defined as follows

$$IC(\%) = 100 \cdot \frac{1}{N_B - 1} \sum_{i=1}^{N_B - 1} |\Delta p(i+1)|$$

where N_B is the total number of heart beats in the registered ECG, $p(i) = k$ where k is the index of the P-wave morphology cluster C_k that classifies the present heart-beat, and $\Delta p(i) = p(i) - p(i-1)$.

3. RESULTS

3.1 Detection of P-wave characteristic points

The protocol used in the study presented in this paper is shown in Table 2. The two first steps in the protocol obtain the onset and end of the P-waves by using the phase-space detection algorithm, see the details in Herreros et al. [2007]. In the first step, the Q points belonging to a sinus QRS complex are found. The associated embedding phase-space was obtained by using a delay $\delta = 30$ ms and $\beta = [0, \ldots, 5]$. In the second step, the embedding phase-space for P-wave onset and end detection is obtained with a delay $\delta = 20$ ms, and $\beta_{Po} = [0, \ldots, 5]$ or $\beta_{Pe} = [-5, \ldots, 0]$, respectively. The sinus Q points obtained in the first step are now used as an indication to find the P-wave onsets and ends. These points are located at the maxima of the inverse distance function and before the previously computed sinus Q points.

The values of the delay δ and embedding dimension N were selected in such a way that the delay δ is sufficiently large to attenuate the high frequency noise and the product $\delta \times N$ is large enough to include the complete wave morphology of the corresponding characteristic point to be detected. The algorithm is quite robust against small changes in these parameters, as is tested in Herreros et al. [2007]. Figure 1 shows a ECG detail of the Q, P onset and P end detection process in $case_3$.

3.2 Classification of P-wave morphologies

In the third step of the protocol of Table 2, the P-waves are extracted from the ECG, filtered with a FIR filter, and rotated to obtain normalized P-waves with zero value for the onset and end points. Figure 2 shows a detail of the result of this process in $case_3$, where the X, Y, Z signals and the spatial magnitude SM are shown. In this figure, all the information of the ECG has been removed, except the normalized P-waves for each beat-heart, that are beat-to-beat orderly represented, one after the other.

The same information is depicted in Figure 3, but now the normalized P-waves for each heart beat are superposed in the same graphic. The indices explained in Section 2.4 are computed by different researchers for the average of these P-waves, assuming that all the P-waves have a similar morphology. Figure 3 shows that this is not the case in $case_3$, where the P-wave clearly changes from beat to beat between two distinct shapes. The use of the average signal could provide spurious information in the corresponding indices. On the other hand, the change in the P-wave morphology is a new phenomenon that has not been completely studied yet and that could report relevant medical information. Consequently, our proposal is to classify the P-waves using a clustering technique, compute the indices for each cluster and study the morphology changes.

The study of the 89 cases, including patient and control subjects, shows that 18 of them have intermittent changes in P-wave morphology. The use of the K-means clustering technique can classify the P-waves of each case into a number of sets. The information from the X, Y, Z leads and SM signal is joined into a vector that comprises the whole P-wave. The K-means clustering algorithm classifies these vectors into two groups. Figure 3 shows all the P-waves for $case_3$ and how they can be classified into two distinct clusters.

The objective of this binary classification is deciding if there is more than one P-wave morphology. Each cluster represents an averaged P-wave morphology. If both clusters are close enough, then there is a unique true P-wave morphology.

The results of this morphology study for three different cases are shown in Figures 4, 5 and 6. In these figures, the P-wave avaraged clusters after the binary classification process are shown in the normalized X, Y, Z and SM signals, in addition the dynamics of the beat-to-beat morphology changes are depicted in the lower graphic where the presence of one cluster is represented by value 0 and the other by value 1 at each heart-beat. Two almost indistinguishable P-wave clusters are found for $case_{41}$, as can be checked in Figure 4. This is the usual case for most of the 89 analyzed cases. Note the fast and almost random changes between both almost indistinguishable clusters, this always happens when there is only one true P-wave morphology and corresponds to a very high value of the IC index that measures the frequency of change

Table 2. Protocol to detect and classify the P-wave morphologies.

(1) Find the sinus Q points using the embedding phase-state algorithm.
(2) Find the P-wave onset and end points associated to sinus Q points using the embedding phase-space algorithm.
(3) Extract, filter and rotate the P-waves.
(4) Classify the P-waves into two clusters using the K-means.
(5) Obtain the cluster means and the dynamics between clusters.

between the obtained P-wave clusters. However, $case_3$ and $case_{33}$ are essentially different as is shown in Figures 5 and 6. Two clearly different P-wave morphologies appear in these cases. In addition, the dynamics of the morphology change is very slow, and each P-wave morphology prevails during a large number of heart beats. For instance, the first 75 heart-beats in $case_3$ corresponds to the first P-wave morphology marked with value 0, the next 100 beats corresponds to the second morphology, marked with value 1, then the P-wave morphology changes again to the first one until the end of the registered heart beats. The IC index takes a small value in these cases. Consequently, there are two different ways to determine if there exists more than one true P-wave morphology. If either the Euclidean distance between the two obtained clusters is small or the IC index is very high then there there exists only one true P-wave morphology, otherwise there exist at least two different P-wave morphologies.

Table 3 shows the 18 cases containing two different P-wave morphologies. The tabulated information for each case comprises: the PR distances, the P-wave length and its standard deviation, the cluster size, the X peak and Z cross-zero time positions, the Z and SM maximum magnitudes and the index of change IC. The values of these indices, with format $(\text{cluster}_1/\text{cluster}_2)$ in Table 3, show large differences between the two morphologies. The index of change IC is small for every case with two morphologies, as it was expected.

Most of the cases with two different P-wave morphologies correspond to healthy individuals. However, more clinical research need to be accomplished in order to understand the causes of the change in the morphology. The protocol developed and reported in this paper establishes a procedure to carry out this research study.

4. DISCUSSION

The phase-space detection algorithm was succesfully used in the detection of the P-wave characteristic points. The algorithm is very simple because only uses time information. This provides very accurate detection results and robustness against noise and variability in the shape of the ECG, as it was shown in Herreros et al. [2007]. The algorithm is semiautomatic, *i.e.*, the user has to choose a reference point for a certain heart-beat, then the algorithm detects all the similar points to the reference, producing only one per beat. All the 89 cases are ECG signals of patients at rest and have less variation that the synthetic signals used in the tests of Herreros et al. [2007]. Therefore, this reinforces the confidence in the accuracy of the obtained detection results.

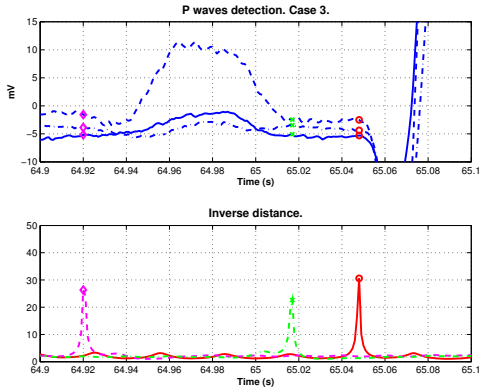

Fig. 1. Detection of P-wave onset, P-wave end and Q event for $case_3$. The upper figure represents the ECG in the three leads. The lower figure represents the modified inverse distance functions for the detection of each event. P-wave onset is marked by a rhombus, P-wave end by a cross and Q event by a circle.

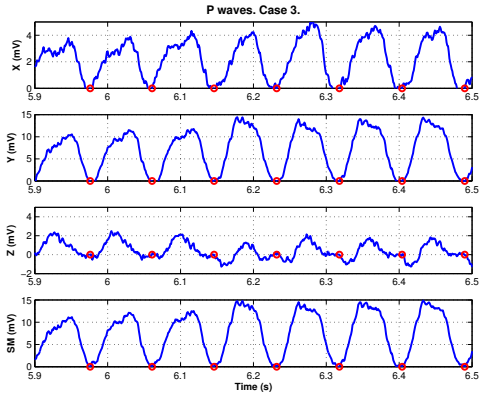

Fig. 2. P-waves detected, isolated, filtered and represented one after the other for $case_3$.

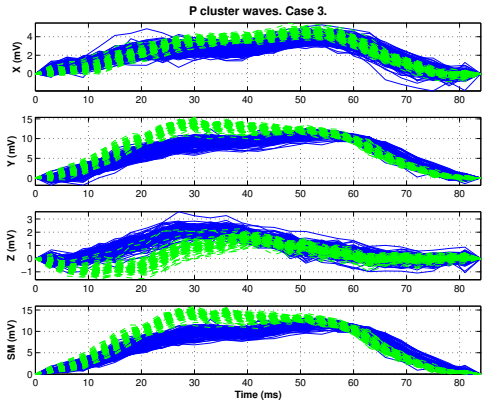

Fig. 3. Superposition of every P-wave of the complete ECG and classification into two clusters for $case_3$. P-waves belonging to the first cluster are depicted in solid line, P-waves belonging to the second cluster are depicted in dashed line.

The selection of the delay δ and embedding dimension N was carried out in order to attenuate the high frequency noise and to include the complete P-wave morphology information in the embedding phase-space vectors, such as it was explained in Herreros et al. [2007].

Table 3. Characteristic index values ($\text{Cluster}_1/\text{Cluster}_2$) for the cases with two different morphologies.

Case	PR	P-wave length	Cluster size	Time X peak	Time Z cross.	Z max.	SM peak	IC(%)
1	124.4 ± 0.8	110.8 ± 0.4	336/37	63/66	60/111	0.4/0.0	16.6/18.0	24.3
2	154.0 ± 2.4	141.7 ± 7.4	48/317	93/66	69/60	4.6/3.6	18.2/9.8	4.2
3	117.8 ± 0.7	84.4 ± 0.5	106/294	51/54	24/12	1.6/2.2	14.2/11.9	6.6
4	192.7 ± 2.7	153.9 ± 2.6	295/62	81/69	66/72	2.0/2.2	19.7/6.8	7.3
7	217.6 ± 5.6	134.7 ± 5.6	74/254	87/66	75/78	4.3/5.3	22.5/17.7	2.7
18	171.0 ± 1.1	123.7 ± 1.1	125/276	75/72	57/51	5.3/6.0	16.1/11.8	4.8
20	151.8 ± 0.8	115.0 ± 0.7	128/185	78/54	108/102	0.1/0.3	15.6/6.8	7.0
33	161.6 ± 0.6	91.1 ± 5.0	91/251	63/45	90/36	0.0/2.2	15.7/14.7	1.6
34	185.7 ± 9.8	131.8 ± 8.6	360/96	90/57	84/75	2.3/2.2	15.3/6.9	10.9
37	214.1 ± 17.4	129.3 ± 15.4	76/340	90/60	78/84	3.9/2.9	12.4/5.8	7.2
43	113.8 ± 7.6	86.9 ± 0.8	114/213	63/42	63/57	0.7/1.2	11.3/9.1	19.7
47	170.5 ± 8.0	138.5 ± 6.8	276/142	69/90	66/69	2.9/3.1	19.1/19.0	6.3
50	224.5 ± 3.8	151.9 ± 4.2	269/56	105/72	75/84	2.9/2.1	15.7/10.0	11.6
51	166.2 ± 0.6	123.1 ± 0.4	200/158	75/51	57/63	4.8/4.2	18.3/10.7	1.3
67	141.3 ± 0.6	112.3 ± 0.7	225/198	87/72	78/87	0.0/0.3	22.3/13.3	1.8
82	138.8 ± 0.6	122.4 ± 0.8	367/62	51/57	51/51	2.3/1.6	11.5/8.3	29.8
85	156.6 ± 6.0	124.5 ± 5.0	172/251	69/51	48/51	0.9/1.6	13.8/10.0	4.9
87	144.2 ± 5.3	132.2 ± 1.3	222/183	81/75	75/87	2.4/1.3	21.4/15.2	2.2

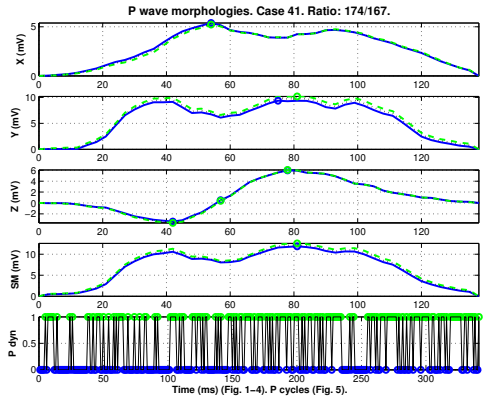

Fig. 4. P-wave cluster means and their dynamic evolution for $case_{41}$. Similar morphologies, fast beat-to-beat changes.

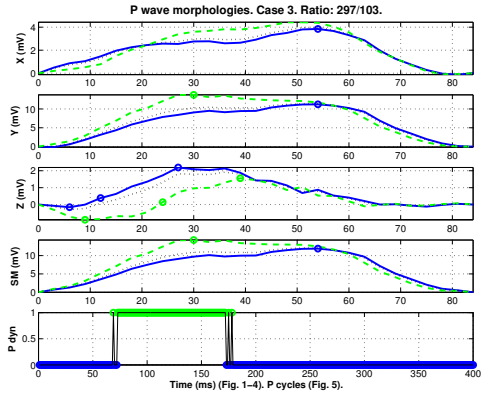

Fig. 5. P-wave cluster means and their dynamic evolution for $case_3$. Different morphologies, slow beat-to-beat changes.

The P-waves that have been detected, isolated and extracted for the 89 ECGs by using the phase-state detection algorithm need to be preprocessed before accomplishing a detailed morphology analysis. The P-waves are filtered and rotated in such a way that their onsets and ends

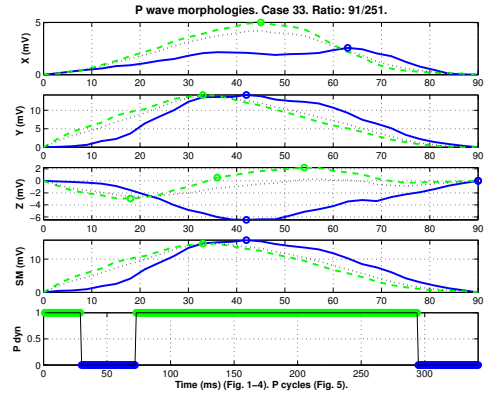

Fig. 6. P-wave cluster means and their dynamic evolution for $case_{33}$. Different morphologies, slow beat-to-beat changes.

attain zero value. Now, a superposition of all the P-waves clearly shows if there exists a morphology change for some of the studied ECG signals. After this study, an interesting phenomenon have been observed for 18 out of the 89 analyzed cases. For these 18 patients, the P-wave presents intermittent morphology changes beat-to-beat. This fact implies two interesting questions: First, are the indices associated to the average P-wave valid for these cases? Second, what is the medical interpretation of these morphology changes?

A binary classification of the P-wave morphologies, using the the K-means clustering algorithm, was accomplished in order to answer the first question. Most cases exhibit only one morphology, but 18 of them have intermittent morphology changes. The indices that characterize each P-wave morphology must be computed for each cluster (averaged P-wave morphology) in order to study atrial conduction defects. Otherwise the results would provide erroneous conclusions. In addition, a new index that measures the beat-to-beat P-wave morphology changes are introduced. The index shows that the cluster changes for these 18 cases are very slow.

The protocol of Table 2 reduces to a figure the P-wave information of 6 minutes of ECG with a minimal loss of information. Figures 4, 5 and 6 are three examples. These figures show two average P-wave clusters (similar or different) and the beat-to-beat changes between then during the ECG. This tool could also be used to study the variability of other ECG waves, such us complex QRS, or T-waves, using a similar protocol.

The most rational explanation of the P-wave morphology changes is that several control subjects change their interatrial conduction delay during the ECG recording, in agreement with the P-wave morphologies noted by Platonov et al. [2000]. A change in the sensor position does not explain this phenomenon, because the P-wave morphology changes are detected in every sensor at the same time, see Figure 2. Clearly, the circumstance that a stable P-wave morphology may abruptly change to another well defined and stable morphology is a new and hitherto unexplored finding. The biological explanation for this finding remains to be further clarified as also the relation to health or disease.

5. CONCLUSIONS

A study of 89 ECGs from patient and control subjects, to detect P-wave morphologies that may predict interatrial delay was carried out. The P-wave information was obtained by an algorithm of detection based on the embedding phase-space approach with very good results. This algorithm was also developed by the same authors of this paper.

A systematic procedure for studing the variability of the P-wave morphology has been developed. This procedure exploits the versatility of the phase-space detection algorithm along with the K-means clustering algorithm. The alternative so far was a tedious process of manual extraction of P-waves. This procedure can be also useful to study the variability of other ECG waves.

The application of this procedure to a collection of ECGs shows intermittent changes in the P-wave morphology for some of them. The P-wave morphology indices detect different electrical activity for each morphology, this fact could be used as a medical predictor of certain pathologies. However, more research is needed in order to develop such a prediction method.

REFERENCES

H.D.I. Abarbanel. The analysis of observed chaotic data in physical system. *Review of Modern Physics*, 65(4): 1331–1392, Oct. 1993.

H.D.I Abarbanel. *Analysis of Observed Chaotic Data Series*. Springer-Verlag, New York, 1996.

M. Bahoura, M. Hassani, and M. Hubin. DSP implementation of wavelet transform for real time ECG waveforms detection and heart rate analysis. *Computer Methods and Programs in Biomedicine*, 52:35–44, 1997.

J.C. Bezdek and S.K. Pal, editors. *Fuzzy model for Patient Recognition*. IEEE PRES, New York, 1992.

C.M. Bishop. *Neural Networks for Pattern Recognition*. Clarendon Press, Oxford, Great Britain, 3th edition, 1997.

J. Carlson, R. Johansson, and S.B. Olsson. Classification of electrodiographic P-wave morphology. *IEEE Transactions on Biomedical Engineering*, 48(4):401–405, 2001.

J. Carlson, R. Havmöller, A. Herreros, P. Platonov, R. Johansson, and B. Olsson. Can orthogonal lead indicators of propensity to atrial fibrillation be accurately assessed from the 12-lead ECG? *Europace*, 7 (Supp. 2):39–48, Sept 2005.

F. Censi, G. Calcagnini, C. Ricci, R.P. Ricci, M. Santini, A. Grammatico, and P. Bartolini. P-wave morphology assessment by a gaussian functions-based model in atrial fibrillation patients. *IEEE Transactions on Biomedical Engineering*, 54(4):663–672, Apr 2007.

J.C Daubert, D. Pavin, G. Jauvert, and P. Mabo. Intra- and ineratrial conduction delay: Implications for cardiac pacing. *Pacing and clinical electrophysiology (PACE)*, 27:507–525, 2004.

R.O. Duda, P.E. Hart, and D.G. Stork. *Pattern Classification*. John Wiley & Sons, 2nd .edition, 2001.

R. Hävmoller, J. Carlson, F. Holmqvist, A. Herreros, C.J. Meurling, B. Olsson, and P. Platonov. Age-related changes in P wave morphology in healthy subjects. *BMC Cardiovascular Disorders*, 7(22), July 2007.

A. Herreros, E. Baeyens, J. Carlsson, R. Johansson, B. Olsson, and J.R. Peran. An Algorithm for Phase-Space Detection of the P Characteristic Points. In *Proceedings of the 29th Annual International Conference of the IEEE Engineering in Medicine and Biology Society*, pages 2004–2007, Lyon (France), August 2007.

H. Kantz and T. Schreiber. *Nonlinear time series analysis*. Cambridge Nonlinear Science Series, 1997.

B.U. Köhler, C. Henning, and R. Orglmeister. The principes of software QRS detection. *IEEE Engineering in Medicine and Biology Magazine*, 21:42–57, Jan./Feb. 2002.

A. Koski. Modelling ecg signals with hidden markov models. *Artificial Intelligence in Medicine*, 8(5):453–71, 1996.

C. Li, C. Zheng, and C. Tai. Detection of ECG characteristic points using the wavelet transfermation. *IEEE Transactions on Biomedical Engineering*, 42:21–28, 1995.

J.P. Martinez, R. Almeida, S. Olmos, and A.P. Rocha. A wavelet-based ECG delineator: Evaluation on standard database. *IEEE Transactions on Biomedical Engineering*, 51(4):570–581, 2004.

P.G. Platonov, S. Yuan, E. Hertevig, O. Kongstad, L.V. Chireikin, and S.B. Olsson. Presence of right atrial conduction disturbance in patients with alone atrial fibrillation. *European Heart Journal*, 19, 1998.

P.G. Platonov, J. Carlson, M.P. Ingemansson, A. Roijer, A. Hansson, L.V. Chireikin, and S.B. Olsson. Detection of inter-atrial conduction defect with unfiltered signal-averaged P-wave ECG in patients with lone atrial fibrillation. *European Pacing and Clinical Electrophysiology (EUROPACE)*, 2:32–41, 2000.

J. S. Sahambi, S. Tandon, and R.K.P. Bhatt. Using wavelet transform for ECG characterization. *Medical & Biological Engineering and Computing*, 16(1):77–83, 1997.

L. Sörnmo and P. Laguna. *Bioelectrical Signal Processing in Cardiac and Neurological Applications*. Elsevier Academic Press, 2005.